Phase synchronization of inhibitory bursting neurons induced by distributed time delays in chemical coupling

Xiaoming Liang,[1] Ming Tang,[1] Mukeshwar Dhamala,[2] and Zonghua Liu[1]

[1]*Institute of Theoretical Physics and Department of Physics, East China Normal University, Shanghai 200062, China*
[2]*Department of Physics and Astronomy, Neuroscience Institute and Center for Behavioral Neuroscience, Georgia State University, Atlanta, Georgia 30032, USA*

Considering the fact that signal transmission time delays between different pairs of synaptically coupled neurons in the brain are different, we study the effects of distributed time delays on phase synchronization of bursting neurons. We consider the case of inhibitory coupled bursting Hindmarsh-Rose neurons and find that distributed time delays in chemical coupling can induce a variety of phase-coherent dynamic behaviors. The critical mean time delay for the emergence of coherent behaviors is inversely proportional to both the coupling strength and the average degree. This phenomenon is robust to nonidentical external inputs and is independent of network topology. A physical theory is formulated to explain the emergence of coherent neuronal activity.

I. INTRODUCTION

Synchronization of neuronal oscillatory activity has been suggested as a mechanism for various cognitive and perceptual processes in the brain such as perceptual grouping, attention-dependent stimulus selection, routing of signals across distributed cortical networks, sensory-motor integration, working memory, and perceptual awareness [1–3]. Abnormal synchronization is also known to be the hallmarks of certain brain disorders, such as epilepsy, schizophrenia, autism, Alzheimer disease, and Parkinson [2]. Synchronized oscillation can occur in neurons from a small brain region to a large-scale network of distributed brain regions. Inhibition plays an important role to induce and balance network oscillations and synchrony both in small- and large-scale brain networks [3–5]. The inhibitory neuronal network consisting of interneurons, coupled to the principal cells, provides the necessary flexibility for the complex operations of the brain [5]. The network module with reciprocal inhibition, a principal building block of various central pattern generators, has been known to generate antiphase oscillations critical for rhythmic motor patterns [6,7]. However, our theoretical understanding of mechanisms for synchronous neural activity patterns in spatially distributed inhibitory neural populations is limited [8]. In particular, the interplay of distributed time delays and inhibitory chemical coupling in phase synchronization of bursting neurons (multitime scale dynamical systems) has not been studied well.

Signal transmission time delays are unavoidable in spatially distributed coupled oscillator systems. Because of different distances and finite signal transmission speeds between different pairs of coupled neurons in the brain, time delays are also spatially distributed. Some experiments have shown that the time delays can scale up to 80 ms in cortical networks [9] and could be distributed in a certain range depending on the type and the location of the neurons in the mammalian neocortex [10,11]. Thus, the influence of time delays on neuronal activity has received a great deal of attention recently [12,13,15,16]. For example, Dhamala *et al.* found neural synchrony enhanced by fixed time delay [12].

Rossoni *et al.* studied the stability of synchronous oscillations in system of neurons with delayed diffusive and pulsed couplings [13]. Lindner *et al.* [14] investigated neuronal firing patterns induced by spatially correlated noise and delayed inhibitory global feedback. Gong and van Leeuwen demonstrated the dynamically maintained spike timing sequences of pulse-coupled neurons under large identical and nonidentical time delays in recurrent networks [15]. Ghosh *et al.* pointed out that the effects of noise and time delays are essential for the emergence of the coherent fluctuations of the brain network [16]. Burić *et al.* recently reported the synchronization of bursting neurons with delayed excitatory chemical (synaptic) synapses [17]. The effects of distributed time delays in inhibitory chemical coupling of bursting neurons have yet to be explored.

In this paper, we investigate the coherent activity patterns induced by distributed time delays in inhibitory, synaptically coupled, bursting Hindmarsh-Rose neurons. We find that the spatiotemporal chaos of the network can be tamed into regular patterns by suitable average delays. The period of the patterns is increased with increasing time delays, which shows that the coupled system goes through a series of periodic-adding bifurcation. This phenomenon is robust to the mismatch of nonidentical external inputs and the network topology.

II. NETWORK MODEL AND SPATIOTEMPORAL PATTERNS

The inhibitory Hindmarsh-Rose neural network model is described by

$$\dot{x}_i = y - ax^3 + bx^2 - z + I_i^{ext} - g_s(x_i - V_s)\sum_{j=1}^{N} g_{ij}\Gamma(x_j),$$
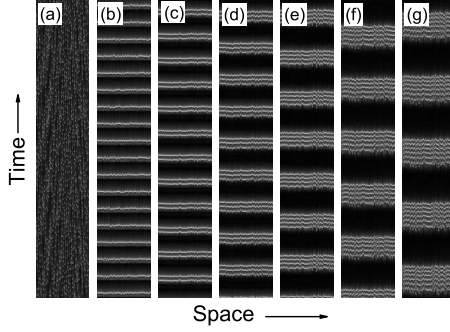
$$\dot{y}_i = c - dx_i^2 - y_i,$$

FIG. 1. Spatiotemporal patterns for $N=100$, $M=1000$, and $g_s=1$ with (a) $\tau=0$, (b) $\tau=8$, (c) $\tau=14$, (d) $\tau=20$, (e) $\tau=30$, (f) $\tau=40$, and (g) $\tau=50$.

$$\dot{z}_i = r[s(x_i - x_0) - z_i], \quad i,j, = 1, \ldots, N, \tag{1}$$

where x is the membrane potential, y is associated with the fast current, Na^+ or Ka^+, and z with the slow current, for example, Ca^{2+}. The parameters are taken as $a=1.0$, $b=3.0$, $c=1.0$, $d=5.0$, $s=4.0$, $r=0.006$, and $x_0=-1.60$. The external inputs are given by I_i^{ext}. The single neuron exhibits a multitime-scaled burst-spike chaotic behavior for $2.92 < I^{ext} < 3.40$. g_s is the synaptic coupling strength and the delayed synaptic coupling function is modeled by the sigmoidal function $\Gamma(x_i) = 1/(1 + \exp\{-\lambda[x_i(t - \tau_{ij}) - \Theta_s]\})$, where Θ_s is the threshold which is chosen such that every spike in the single neuron bursting can reach the threshold. We here take $\Theta_s = 0$ and $\lambda = 30$. V_s is the reversal potential; its sign determines the synapse whether excitatory or inhibitory. In this paper, we consider the case of inhibitory and let $V_s = -1.8$. τ_{ij} is the conduction delays between node i and j. $\mathbf{G} = (g_{ij})$ is the coupling matrix: $g_{ij} = g_{ji} = 1$ if there is a link between neurons i and j, $g_{ij} = g_{ji} = 0$ otherwise, and $g_{ii} = 0$. In our study, the network is constructed by adding $M-N$ random links to a circular ring of N nodes, i.e., the total number of links is M and the average degree is $K = 2M/N$. The corresponding distributed time delays between coupled neurons are set as $\tau_{ij} = \text{int}[\tau(1 + c\xi)]$, where $\text{int}[.]$ denotes the integer part of $[.]$; ξ is a Gaussian white noise with zero mean and unitary standard deviation. τ denotes the mean value of delay and $c\xi$ denotes the fluctuations of distance in realistic natural systems and satisfy $1 + c\xi > 0$. For simplicity, we let $c = 0.1$.

We first consider the case of identical external input with $I_i^{ext} = 3.2$ and $M = 1000$. Our numerical simulations show that in the given set of parameters, the coupled systems will be chaotic and unsynchronized when $\tau = 0$ [see Fig. 1(a)]. However, we surprisingly find that when τ becomes nonzero, i.e., τ_{ij} has a distribution, it is possible for the network to emerge regular spatiotemporal patterns, [see Figs. 1(b)–1(d)]. From Figs. 1(b)–1(d), it is easy to see that all the oscillators have the same behavior, indicating that they are synchronized. Moreover, one can see that with the increase of τ, the synchronized pattern changes from period 1 in (b) to period 2 in (c), then to period 3 in (d), and to higher periods as shown in Figs. 1(e)–1(g).

In order to get more detailed insight of the ordered patterns in Fig. 1, we introduce an indicator of the average membrane potential
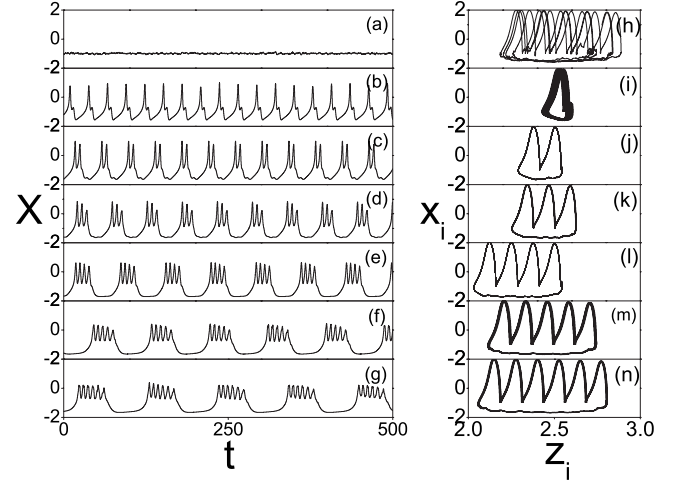

FIG. 2. (Left panels) Time series of the indicator X with $\tau=0$ in (a), $\tau=8$ in (b), $\tau=14$ in (c), $\tau=20$ in (d), and $\tau=30,40,50$ in (e)–(g), respectively. (Right panels) The corresponding trajectories of the left panels for a randomly chosen neuron. The value of g_s is 1.

$$X = \frac{1}{N}\sum_{i=1}^{N} x_i(t). \tag{2}$$

If the neurons are weakly correlated, for example, they burst at different times, X fluctuates irregularly with small amplitudes. Instead, X shows regular dynamics if all neurons burst coherently. We find that the different patterns in Fig. 1 correspond to different behaviors of X. The left panels of Fig. 2 show how X changes with t, which corresponds to Figs. 1(a)–1(d). It is easy to see that the value of X fluctuates slightly around -1 in (a) with $\tau=0$, indicating that the neurons are not bursting in phase. And X shows a sequence of large amplitude spike in (b) with $\tau=8$, indicating that the neurons spike at approximately the same time. When τ is increased to $\tau=14$ in (c), the burst becomes two spikes. When τ is further increased to $\tau=20$ in (d), the burst becomes three spikes. Higher τ's result in higher periods [Figs. 1(e)–1(g)].

The right panels of Fig. 2 show the corresponding trajectories of the left panels for a randomly chosen neuron. Comparing Fig. 2(a) to Fig. 2(h), we see that each neuron is in a chaotic state and bursts randomly, resulting in the spatiotemporal chaos in Fig. 1(a). In the same way, we can explain the approximate period 1, period 2, and period 3 spikings in Figs. 2(i)–2(k). We also notice that the phase trajectories shown in Figs. 2(h)–2(k) are nonidentical to different neurons, indicating the influence of different degree of each neuron [18]. In addition, it is worthwhile to mention that this ordered phenomenon caused by distributed delays is similar to the cases of spike adding in Ref. [19] induced by increasing coupling strengths.

As shown in Figs. 2(b)–2(d), there exists an ordered behavior although the neurons are not completely synchronized. We will introduce an order parameter to describe this collective behavior. Let us define a phase for each neuron as follows:
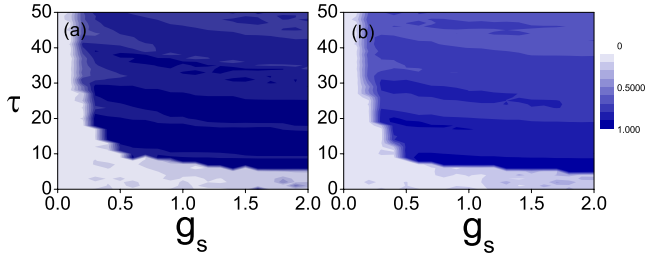
FIG. 3. (Color online) Order parameter $\bar{R}$ for different pairs of coupling strength g_s and time delay τ with $N=100$ and $M=1000$. (a) $I_i^{ext}=3.2$; (b) $I_i^{ext} \in (2.92, 3.40)$.

$$\varphi_i(t) = 2\pi \frac{t - T_{i,k}}{T_{i,k+1} - T_{i,k}},$$

$$T_{i,k} \leq t \leq T_{i,k+1}, i = 1, \dots, N, \quad (3)$$

where $T_{i,k}$ represents the time of spiking, i.e., the moment with the maximum of $x_i(t)$. The order parameter of phase can be written as

$$z(t) = R(t)\exp[i\Phi(t)] \equiv \frac{1}{N}\sum_{j=1}^{N} \exp[i\varphi_j(t)]. \quad (4)$$

where $R(t)$ and $\Phi(t)$ are the amplitude and angle, respectively. The time-averaged order-parameter magnitude is

$$\bar{R} = \lim_{T \to \infty} \sum_{t=1}^{T} R(t), \quad (5)$$

where $\bar{R}$ would be zero for weak correlation and tends to unity for a complete phase synchronization. Figure 3(a) shows $\bar{R}$ for different pairs of coupling strength g_s and time delay τ. Here, we find that $\bar{R}$ suddenly becomes unity when time delay and coupling strength is over a pair of critical values τ^* and g_s^* [see Fig. 3(a)] which correspond to the complete phase synchronization. Moreover, from Fig. 3(a), it is easy to see that there is a relationship between τ^* and g_s^*, i.e., $\tau^* \times g_s^* \approx$ const. That is, for a fixed g_s, we can tame chaos with sufficient time delay and for a fixed τ, we can tame chaos with sufficient coupling strength. Is this phenomenon robust to the links M? Figure 4(a) shows the results for $M=1000$, 2000, and 3000, respectively, which correspond to the average degrees $K=20$, 40, and 60. Interestingly, we find that for a fixed g_s, the threshold τ^* is inversely proportional to the average degree K. To see it clearer, we plot the $2\tau^*$ of $K=40$ and $3\tau^*$ of $K=60$ with the τ^* of $K=20$ together [see the inset of Fig. 4(a)]. Obviously, all the three curves are approximately overlapped, indicating the invariance of normalization on the average degree K. A similar result holds for the relationship between g_s^* and K for fixed τ. Furthermore, we check the influence of network size on the thresholds. We increase N from 100 to 200 and then to 500 but keep the average degree as constant $K=20$. Figure 4(b) shows the results. It is easy to see that the three curves are approximately overlapped, indicating that the correlated patterns are robust to network size.
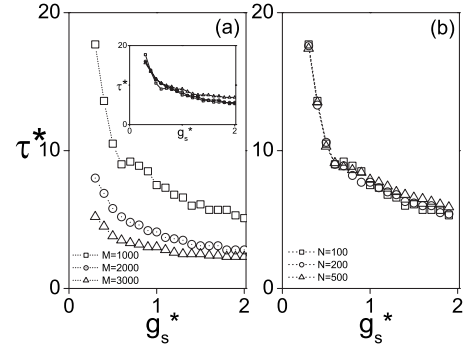

FIG. 4. The relationship between τ^* and g_s^* for different number of links M and network size N. (a) τ^* for $N=100$, $M=1000$, 2000, and 3000. [Inset of (a)] The normalized τ^* based on $M=1000$. (b) τ^* for $N=100$ and $M=1000$ (squares), $N=200$ and $M=2000$ (circles), and $N=300$ and $M=3000$ (triangles).

Because of the diversity of degree distribution in networks, different individual oscillators may get different external inputs. Here, we look at whether the observed phenomena are robust to the nonidentical signal I_i^{ext}. We let I_i^{ext} be random uniformly distributed from the interval (2.92, 3.40) in which individual oscillators are all chaotic. Surprisingly, we have observed the similar results as shown in Figs. 1–3. Here, we plot the dependence of the order parameter $\bar{R}$ on g_s and τ in Fig. 3(b). It is easy to find that Fig. 3(b) is very similar to Fig. 3(a), indicating the robust to nonidentical external inputs I_i^{ext}.

We also look at the influence of parameter c and the network topology on the coherent behaviors. We find that the observed phenomenon remains for other values of c except the threshold of average delay τ^* is increased when we increase c. However, the Gaussian distribution of time delay becomes flat with large c, which is similar to the uniformly distribution, and weakens the effect of time delay.

III. PHASE-REDUCED MODEL TO EXPLAIN ORDERED PATTERNS

We use a phase-reduced model to shed light on the effect of distributed time delays. The advantage of phase-reduced model is that one can carry out the analytical calculations [20,21]. For the sake of simplicity, we consider simply the single-spike firing pattern of single spike to carry out theoretical analysis. That is, we consider the case in which each neuron has the firing time series similar to Fig. 2(b) but spiking incoherently when the parameters (τ^* and g_s^*) are lower than the thresholds.

The phase-reduced model of Eq. (1) can be assumed as

$$\dot{\theta}_i = \omega_i - \varepsilon \sum_{j=1}^{N} g_{ij} H[\theta_j(t - \tau_{ij}) - \theta_i(t)], \quad i = 1, 2, \dots, N,$$

$$(6)$$

where ω_i are natural frequencies, $\theta_i(t)$ the phases of individual neurons, and $-\varepsilon$ the inhibitory coupling strength. $H(\theta)$ is a 2π-periodic function and estimated by phase reduction

method for pairwise interaction. In general, $H(\theta)$ can be approximated by a few Fourier components $H(\theta) = \Sigma_{n=0}^{3}[a_n \cos(n\theta) + b_n \sin(n\theta)]$ [20]. Here, we choose the simplest possible periodic coupling function $H(\theta) = \sin(\theta)$ which is widely used in many studies [21–23]. Then, Eq. (6) becomes

$$\dot{\theta}_i = \omega_i - \varepsilon \sum_{j=1}^{N} g_{ij} \sin[\theta_j(t - \tau_{ij}) - \theta_i(t)]. \tag{7}$$

When all the oscillators are synchronized, they will have the same frequency $\Omega = \omega_i + \varepsilon \Sigma_{j=1}^{N} g_{ij} \sin(\Omega \tau_{ij}), i = 1, 2, \dots, N$. As τ_{ij} satisfies the Gaussian distribution with mean τ and standard deviation $\sigma = c\tau$, we have

$$\Omega \approx \omega_i + \varepsilon K \frac{\sqrt{2\pi}}{\sigma\pi} \int_0^\infty \exp\left(-\frac{(\tau' - \tau)^2}{2\sigma^2}\right) \sin(\Omega\tau') d\tau'$$

$$= \omega_i + \varepsilon K \exp\left(\frac{-(c\tau\Omega)^2}{2}\right) \sin(\Omega\tau).$$

Letting $\varepsilon e^{-(c\tau\Omega)^2/2} \equiv \varepsilon'$, we obtain

$$\Omega \approx \omega_i + \varepsilon' K \sin(\Omega\tau), i = 1, 2, \dots, N. \tag{8}$$

It is easy to see that ε is inversely proportional to K for fixed τ. As K is proportional to M, thus ε is inversely proportional to M, confirming Fig. 4(a). Then we let ω_i be $\frac{\pi}{16}$ or distributed in the range $(-\frac{\pi}{8}, \frac{\pi}{8})$ and apply the same delay distributions as in Eqs. (1)–(7). Here, ω_i is not specific and can be set as other values. Using Eq. (5), we calculate the coherent
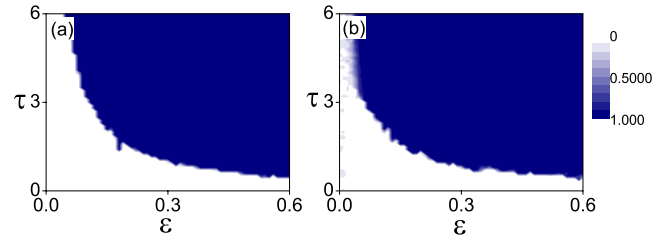

FIG. 5. (Color online) Order parameter $\bar{R}$ for different pairs of coupling strength ε and time delay τ in a network with $N = 100$ and $M = 1000$. (a) $w_i = \frac{\pi}{16}$. (b) $w_i \in (-\frac{\pi}{8}, \frac{\pi}{8})$.

indicator $\bar{R}$ and find the similar trend with Fig. 3 [see Fig. 5 for $N = 100$ and $M = 1000$ in Eq. (7)]. Thus, the phase-reduced model (7) explains the coherent behaviors of the Hindmarsh-Rose neurons observed in Fig. 3.

IV. CONCLUSIONS

We have studied the effects of distributed time delays and coupling strengths on the collective behaviors of synaptically coupled inhibitory Hindmarsh-Rose neurons. We find that the time delays induce different ordered patterns and the period increases with the increasing value of average delay via period-adding bifurcation. The critical values of coupling strength and time delay have an inverse relationship when neurons become phase synchronized. A simple phase-reduced model explains the occurrence of these time-delay-induced coherent behaviors.

[1] F. Varela, J. P. Lachaux, E. Rodriguez, and J. Martinerie, Nat. Rev. Neurosci. **2**, 229 (2001).
[2] P. J. Uhlhaas and W. Singer, Neuron **52**, 155 (2006).
[3] W. Singer, Scholarpedia J. **2**, 1657 (2007).
[4] I. Mody and R. A. Pearce, Trends Neurosci. **27**, 569 (2004).
[5] G. Buzsáki, K. Kaila, and M. Raichle, Neuron **56**, 771 (2007).
[6] R. L. Calabrese, Curr. Opin. Neurobiol. **5**, 816 (1995).
[7] P. S. G. Stein, S. Grillner, A. I. Selverston, and D. G. Stuart, *Neurons, Networks, and Motor Behavior* (MIT, Cambridge, MA, 1997).
[8] S. A. Campbell, in *Handbook of Brain Connectivity*, edited by A. R. McIntosh and V. K. Jirsa (Springer, Berlin, 2007), Vol. 65.
[9] E. R. Kandel, J. H. Schwartz, and T. M. Jessell, *Principles of Neural Science*, 3rd ed. (Elsevier, New York, 1991).
[10] H. A. Swadlow, J. Neurophysiol. **68**, 605 (1992).
[11] H. G. Schuster and P. Wagner, Prog. Theor. Phys. **81**, 939 (1989).
[12] M. Dhamala, V. K. Jirsa, and M. Ding, Phys. Rev. Lett. **92**, 074104 (2004).
[13] E. Rossoni, Y. Chen, M. Ding, and J. Feng, Phys. Rev. E **71**,

061904 (2005).
[14] B. Lindner, B. Doiron, and A. Longtin, Phys. Rev. E **72**, 061919 (2005).
[15] P. Gong and C. van Leeuwen, Phys. Rev. Lett. **98**, 048104 (2007).
[16] A. Ghosh, Y. Rho, A. R. McIntosh, R. Kötter, and V. K. Jirsa, PLOS Comput. Biol. **4**, e1000196 (2008).
[17] N. Burić, K. Todorovic, and N. Vasovic, Phys. Rev. E **78**, 036211 (2008).
[18] I. Belykh, E. de Lange, and M. Hasler, Phys. Rev. Lett. **94**, 188101 (2005).
[19] Y. Shen, Z. Hou, and H. Xin, Phys. Rev. E **77**, 031920 (2008).
[20] R. F. Galán, G. Bard Ermentrout, and N. N. Urban, Phys. Rev. Lett. **94**, 158101 (2005).
[21] T.-Wook Ko and G. Bard Ermentrout, Phys. Rev. E **76**, 056206 (2007).
[22] M. K. Stephen Yeung and S. H. Strogatz, Phys. Rev. Lett. **82**, 648 (1999).
[23] Z. Liu, Y.-C. Lai, and F. C. Hoppensteadt, Phys. Rev. E **63**, 055201(R) (2001).